

OPERATIONAL LIMITS ASSESSMENT FOR HIGH-ALTITUDE LONG-ENDURANCE UAVS CONSIDERING PROPELLER ICING EFFECT

Yonghwan Kim¹, Jeong-Ho Shin², Chanju Woo², Chankyu Son², and Kwanjung Yee¹

¹ Dept. of Aerospace Engineering, Seoul National University 1

Abstract

High-altitude long-endurance (HALE) unmanned aerial vehicles (UAVs) operate in the stratosphere above 15 km, relying on long wingspans, low speeds, and lightweight designs with propeller propulsion. However, these aircraft are vulnerable to icing during ascent, which can alter aerodynamic performance and increase weight due to ice accumulation. Previous studies have primarily focused on icing effects on the fuselage and wings, overlooking the critical impact on the propeller. This study addresses this gap by conducting three-dimensional icing simulations, incorporating the propeller blades using the Multiple Reference Frame (MRF) method. Separate simulations are conducted for each component (fuselage, wings, and propeller) due to the propeller's relatively small radius compared to the wingspan. The results demonstrate that propeller icing significantly affects required battery capacity and DC motor performance, imposing operational limitations. Therefore, considering propeller icing is essential when evaluating the operational limits of HALE UAVs under icing conditions.

Keywords: High-Altitude, Long-Endurance Unmanned Aerial Vehicle (HALE UAV), UAV Icing, Numerical Simulation Method, Performance Degradation Analysis, Operational Limit

1. Introduction

High-altitude long-endurance (HALE) aircraft are unmanned aerial vehicles (UAVs) that perform long-term missions in the stratosphere at altitudes above 15 km. Due to their specialized mission, these aircraft are characterized by a long wingspan, low speed and an ultra-lightweight design with propeller propulsion. However, these features make them vulnerable to the icing conditions they may encounter during the climb phase of their flight. In particular, ice accumulation on the surface of these aircraft persists for long periods of time, resulting in changes to the surface roughness, an increase in the total mass and a reduction in aerodynamic performance.

Several studies have analyzed the effects of icing on HALE UAVs [1–4]. Vogel [1] found that ice accumulation on the wings of HALE aircraft can reduce the rate of climb (ROC), which can impact operations. Son [4] identified the icing conditions that HALE UAVs may encounter during flight and predicted the icing geometry without propeller. He then evaluated performance changes and determined operational limits based on the ratio of required battery capacity to a given total battery capacity [4].

Previous studies of icing effects on HALE UAVs have primarily focused on the effects of icing on the fuselage, ignoring the effects of icing on the propeller, which is small in size compared to the long wingspan [4]. However, the propeller section has a relatively short chord length and large inflow velocity due to rotation, which will cause more severe geometry changes, making it more susceptible to icing. Furthermore, if the propeller efficiency decreases due to icing, higher RPMs may be required, which may affect the efficiency of the DC motors connected to the propeller. Therefore, it is essential

² Dept. of Unmanned Aircraft Systems, Cheongju University 2

to consider propeller icing when analyzing the effects of icing on HALE UAVs.

The objective of this study is to determine the operational limitations of the HALE UAV in the context of propeller icing effects. To this end, three-dimensional (3D) icing simulations are conducted for the entirety of the airframe and the propeller. In particular, 3D icing simulations employing the Multiple Reference Frame (MRF) method are performed for the propeller blade. Independent icing simulations are executed for the fuselage and wings and the propeller under each icing condition. In reality, there is interaction between the propeller and the fuselage or wing components. However, in this study, independent icing simulations are performed for each with the assumption that the radius of the propeller is small, approximately 12% of the wing span. This assumption is made in order to ignore the impact of propeller icing on the fuselage and wing.

The icing geometry obtained from the icing simulation analysis was used for the performance degradation analysis. To demonstrate the impact of propeller icing, a comparison was made with a method that did not consider propeller icing. Furthermore, the results of the degradation analysis were employed to ascertain the mission feasibility through the total battery capacity and DC motor specification required for the climb phase based on the given mission profile. This study confirmed that the impact of propeller icing is significant when evaluating the operational limits of the HALE UAV under given icing conditions.

2. Numerical Methods

To assess the operational limits of HALE UAVs in the context of propeller icing effects, it is essential to consider the selection of an appropriate HALE UAV model, the analysis of icing, and the evaluation of performance degradation. In this study, computational fluid dynamics (CFD) was employed for both icing analysis and performance degradation analysis. The overall analysis procedure is depicted in Figure 1.

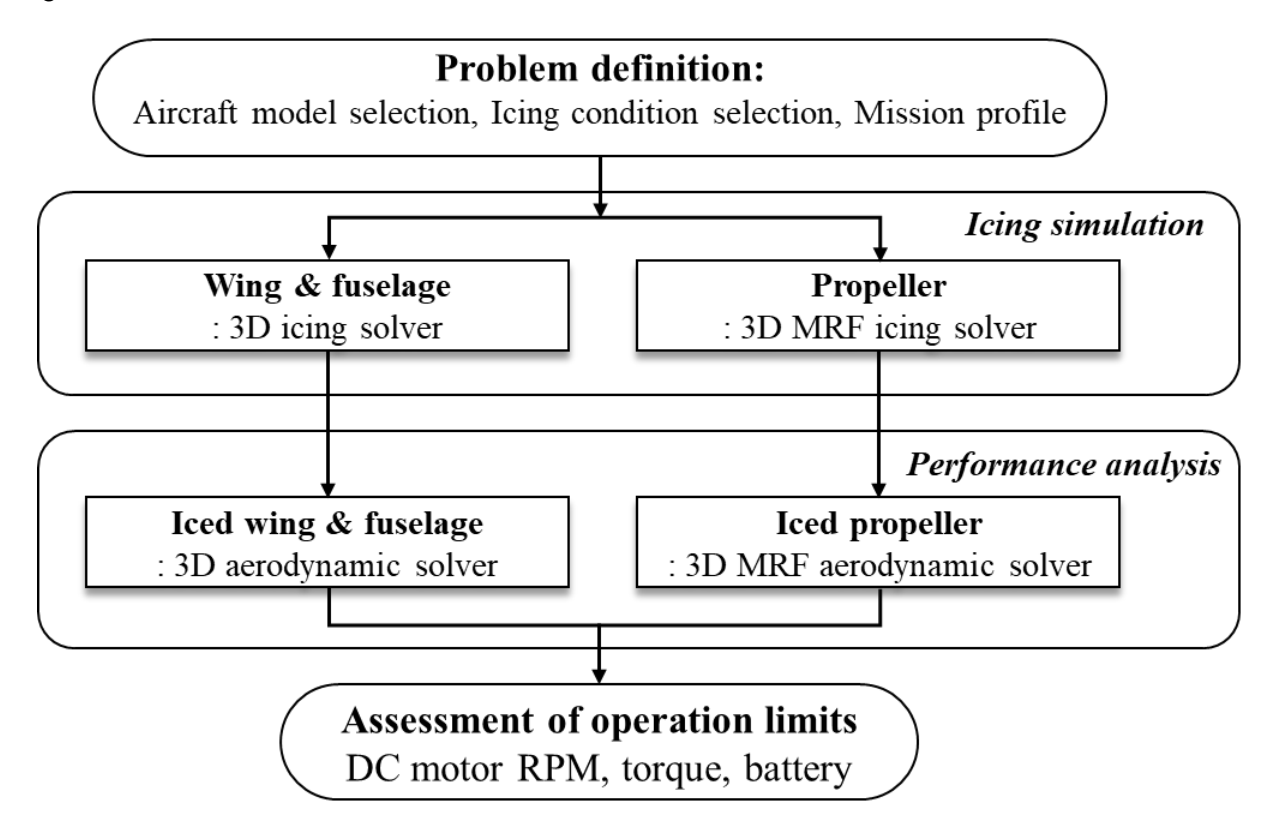


Figure 1 – Flow chart for Determination of operation limit.

2.1 Problem Definition

The initial step, designated the problem definition phase, entails the selection of the aircraft model, the identification of icing conditions, and the determination of the duration of exposure to icing. The icing conditions are based on Appendix C of the Federal Aviation Regulations (FAR), which specifies parameters related to icing. The distance exposed to icing is also calculated using the mission profile of the selected aircraft and the identified icing environment. This is done by dividing the duration of exposure to icing by the aircraft's cruise speed.

2.2 Icing Simulation

In this study, ICEPAC [5] was employed using OpenFOAM, an open-source computational fluid dynamics (CFD) analysis tool, to predict the icing geometry on the fuselage, wing, and propeller, and to analyze its impact on performance degradation. OpenFOAM enables the execution of CFD analyses based on the Navier-Stokes equation (N-S equation), as well as additional calculations for other physical analyses based on the finite volume method (FVM). This facilitates the development of solvers for flow field analyses, such as ICEPAC [5].

The 3D MRF method, as implemented by ICEPAC [5], was employed to analyze icing on a rotating propeller [7-11]. The MRF method is a flow field analysis technique that can obtain steady-state analysis results quickly by treating the blade and the surrounding area as a stationary grid system. This is achieved by converting the rotation effect of the blade into the coordinate system. The method considers three-dimensional and rotational effects by incorporating the Coriolis and centrifugal forces generated during the coordinate transformation into the momentum conservation equation [7].

In the context of MRF analysis of icing on rotating blades, it is necessary to apply both Coriolis and centrifugal forces to both the flow field and the droplet field. Additionally, in the thermodynamics module, the wall shear stress of the flow field with rotation effects can be applied to accurately reflect the three-dimensional propeller and rotational effects.

2.3 Performance Analysis

The performance analysis is conducted separately for the wing-body section and the propeller. Firstly, for the wing and body sections, grid remeshing is performed using the iced geometry predicted by the full three-dimensional computational fluid dynamics (CFD) simulation to ascertain changes in lift and drag coefficients. Additionally, the extra weight resulting from ice accumulation on the surface is also considered. The performance analysis for the propeller is conducted using the 3D MRF method. Similar to the wing and body, grid remeshing is performed on the predicted iced propeller geometry. The thrust and power coefficients are then obtained from the pressure distribution to determine how they change with icing. The change in efficiency can also be demonstrated by calculating the propeller efficiency using the obtained coefficients in Eq. (1). Additionally, the weight of the ice on the surface of the propeller is calculated.

$$\eta_{propeller}(t) = \frac{C_T(t) \cdot J}{C_p(t)} \tag{1}$$

2.4 Assessment of Operation Limits

This step evaluates the operational limitations of a given mission geometry by assessing parameters such as the required battery capacity, rpm of the DC motor, and torque, depending on the mission geometry. To determine these values, the forces acting on the aircraft are calculated based on the aerodynamic performance of the HALE UAV obtained in the previous step as shown in Figure 2, and then the required thrust to operate the aircraft is calculated. The lift coefficient, drag coefficient, propeller thrust coefficient, power coefficient, and propeller efficiency for the fuselage and wings are influenced by changes in geometry resulting from icing. Additionally, the weight gain due to ice affects

the magnitude of the required lift. In icing conditions, these values undergo temporal changes, and in this study, it is assumed that these changes occur linearly over time.

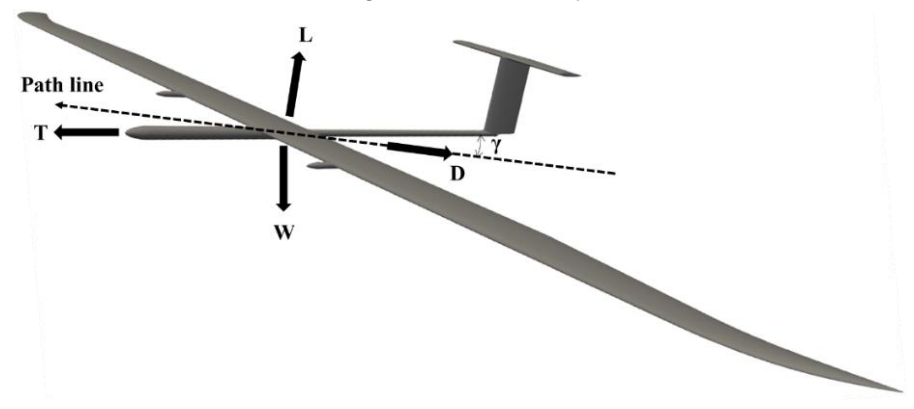


Figure 2 – Forces on the fuselage and wing of HALE UAV.

$$D(t) = C_{D,0}(1 + \Delta C_D \cdot t/t_{ice}) \cdot 1/2 \cdot \rho(t)U(t)^2 \cdot A$$
(2)

$$L(t) = C_{L,0}(1 + \Delta C_L \cdot t/t_{ice}) \cdot 1/2 \cdot \rho(t)U(t)^2 \cdot A$$
(3)

$$W(t) = M(1 + \Delta M \cdot t/t_{ice}) \cdot g \tag{4}$$

$$T(t) = L(t) \cdot \sin(\gamma) + D(t) \cdot \cos(\gamma) \tag{5}$$

The thrust required for propulsion is calculated using Eq. (6), which considers the aircraft speed and the efficiency (η_{tot}) required for the operation.

$$P(t) = T(t) \cdot V(t) / \eta_{tot}(t) \tag{6}$$

$$\eta_{tot}(t) = \eta_{battery}(t) \cdot \eta_{propeller}(t) \cdot \eta_{motor}(t) \cdot \eta_{control}(t)$$
(7)

In general, as the altitude of a high-altitude long-endurance (HALE) unmanned aerial vehicle (UAV) increases, the air density decreases, leading to an increase in aircraft speed, required revolutions per minute (RPM), and a decrease in required torque. *n* represents RPS (revolutions per second). The required RPM and torque are derived from the propeller thrust coefficient and torque coefficient, as follows:

$$RPM(t) = \sqrt{\frac{T(t)}{2 \cdot \rho \cdot C_{T,0} (1 + \Delta C_T \cdot t/t_{ice}) \cdot D^4}} \cdot 60$$
 (8)

$$Q(t) = C_{P,0}(1 + \Delta C_P \cdot t/t_{ice}) \cdot \rho \cdot n^2 \cdot D^5/2\pi$$
(9)

Integrating the calculated power over the duration of the flight provides the amount of energy required to reach the target altitude (W_{reg}).

$$W_{req} = \int P(t)dt \tag{10}$$

For an aircraft with a constant rate of climb, the relationship between RPM, torque(Q(t)), and required power (W_{reg}) over time can be expressed as a function of altitude.

3. Results

3.1 Model Descriptions and Problem Setting

The icing simulation environment is set up using the EAV-3 HALE UAV [12-13], developed by the Korea Aerospace Research Institute (KARI). The specifications of this aircraft are summarized in Table 1.

Table	1 –	· EAV-3's	specification	[13].
-------	-----	-----------	---------------	-------

Property	Value		
Weight(kg)	46.5		
Rate of climb(m/s)	0.75		
$W_{prov}(kJ)$	37,440		

The determination of icing conditions relies on parameters defined in the US Federal Aviation Regulations (FAR) Appendix C [14]. This regulation establishes correlations among key parameters affecting icing formation, such as liquid water content (LWC), mean volume diameter (MVD), and temperature. As shown in Table 2, three specific conditions were simulated in this study for clouds containing supercooled droplets. The same MVD was used to examine the effects of varying LWC and temperature.

Table 2 – Selected icing conditions.

Table 2 – delected foling conditions.					
Case	LWC(g/m3)	T(°C)	MVD(μm)		
1	0.2	-30	15		
2	0.456	-14.25	15		
3	0.735	-5	15		

The duration of icing exposure is established based on FAR Appendix C [14] and the mission profile of the HALE UAV, as shown in Figure 3. The HALE UAV used in this study has a target mission altitude of 18 kilometers, which places it within the stratosphere. Icing occurs when the air temperature is below 0 degrees Celsius. Therefore, the minimum altitude for icing conditions was set at 2.3 kilometers, where the standard air temperature reaches 0°C. Additionally, the maximum altitude for icing conditions was set at 6.7 kilometers to encompass the highest altitude of clouds expected to be encountered by the HALE UAV.

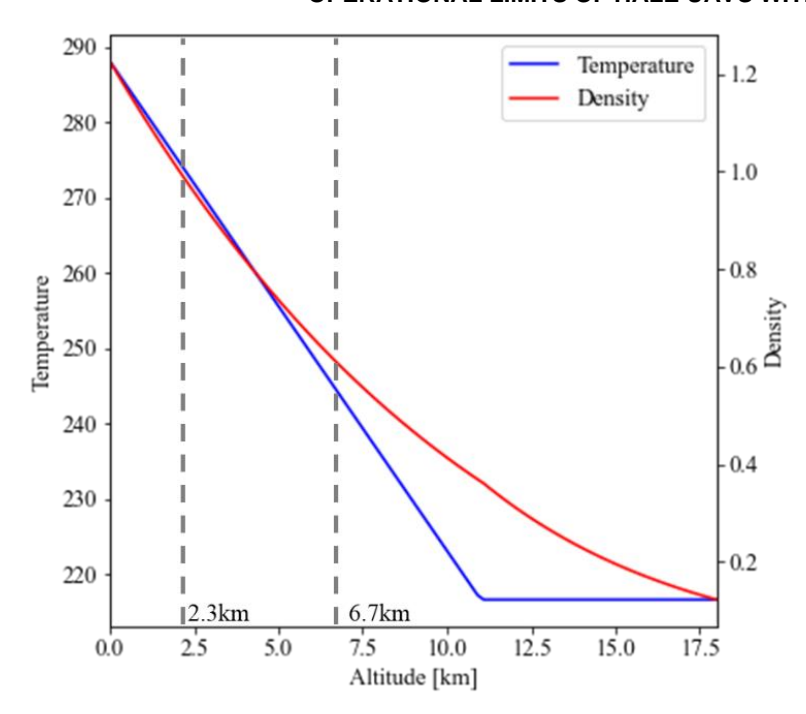


Figure 3 – icing exposure range of HALE UAV.

Given that the aircraft experiences icing conditions during its ascent from 2.3 to 6.7 kilometers at a constant climb rate of 0.75 meters per second, the total icing exposure time was determined to be approximately 1.63 hours.

3.2 Icing Simulations

To analyze the effect of icing on the EAV-3 HALE UAV selected for this study, a simulation analysis will be conducted. The first step involves constructing a 3D grid for the simulation of the fuselage and wing. Figure 4 depicts the grid utilized in this simulation. The surface grid consists of 420,000 unstructured cells, while the volumetric grid comprises 280 million cells. Additionally, 30 prism layers were generated with a growth rate of 1.2.

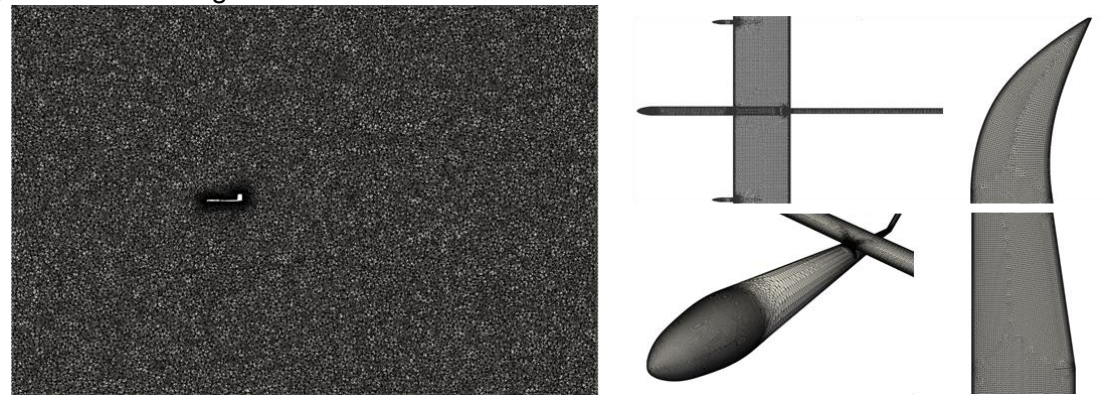


Figure 4 – 3D grid generation of EAV-3's fuselage and wing.

In this study, a small Median Volume Diameter (MVD) was used, which led to a lower impingement limit for the droplets. This condition allowed the droplets to follow the airflow more closely, resulting in a reduced collection efficiency. As a consequence, there was less ice accumulation observed on the fuselage and wings, as illustrated in Figure 5, indicating a diminished impact from icing.

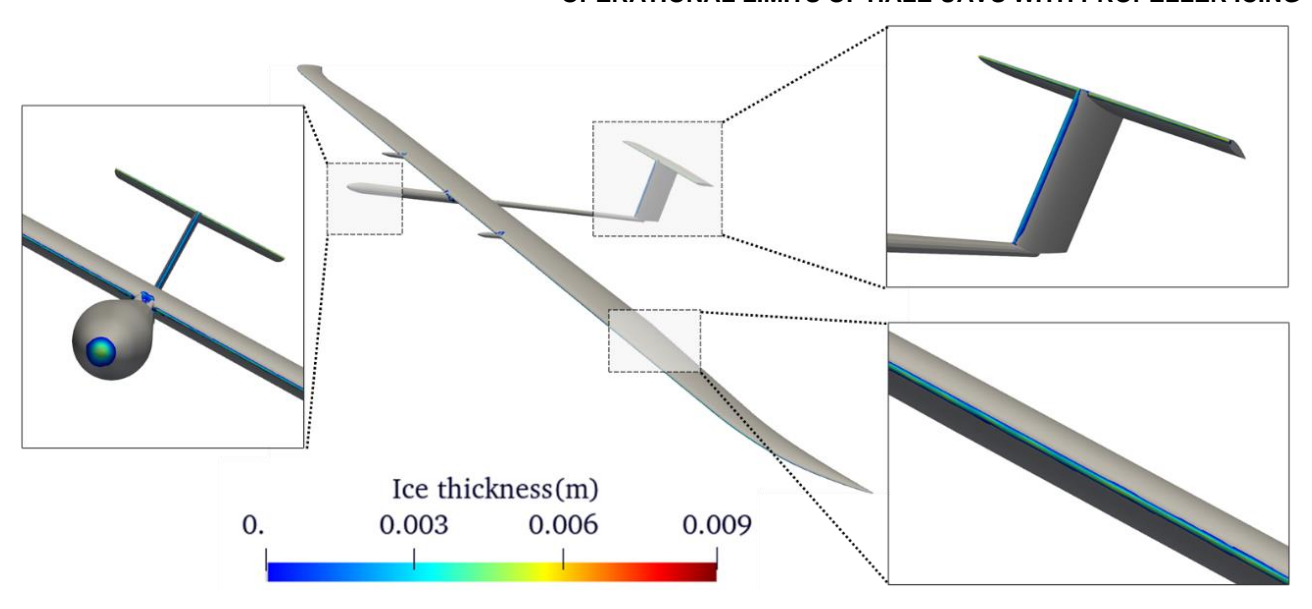


Figure 5 – Icing prediction result of fuselage and wing (Case 1).

Also, a grid is constructed for the 3D simulation analysis of the propeller. Figure 6 illustrates the grid utilized in this simulation. Since the analysis will employ the Multiple Reference Frame (MRF) method, it is crucial to define a region of rotation around the propeller. The grid consists of a total of 11 million unstructured grid cells.

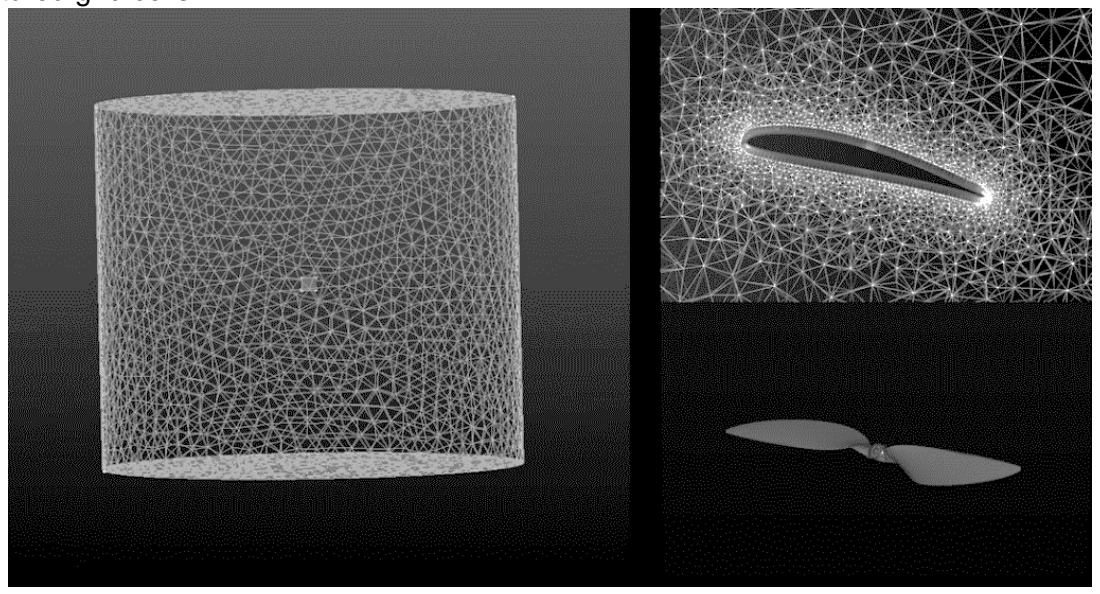


Figure 6 – 3D MRF grid generation of EAV-3's propeller.

The results of the Multiple Reference Frame (MRF) analysis for the propeller are illustrated in Figure 7. The MRF analysis demonstrates that the rotating flow around the propeller causes the droplet field to rotate synchronously with it. As a result of this analysis, the icing analysis result is presented in Figure 8 and 9. Figure 8 and 9 illustrate the ice geometry obtained from the MRF analysis by sections based on the radius. To ensure the reliability of the results, they are compared with the 2D analysis results obtained through Blade Element Momentum Theory (BEMT) analysis.

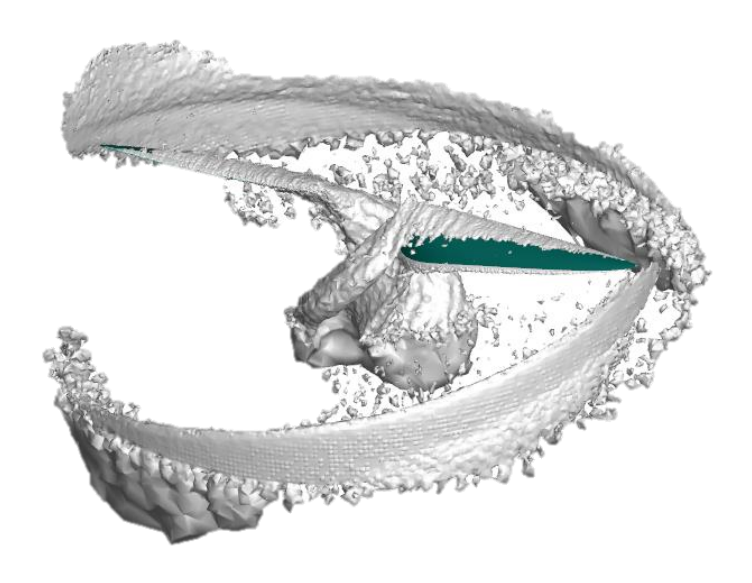


Figure 7 – 3D MRF result of EAV-3's propeller: droplet density (Case 1).

In Case 1, which is a rime case, the temperature is low and the liquid water content is relatively low. Conversely, Case 3 shows glaze ice, characterized by higher temperatures and higher liquid water content. It can be seen that both analytical results show similar ice geometry in all conditions.

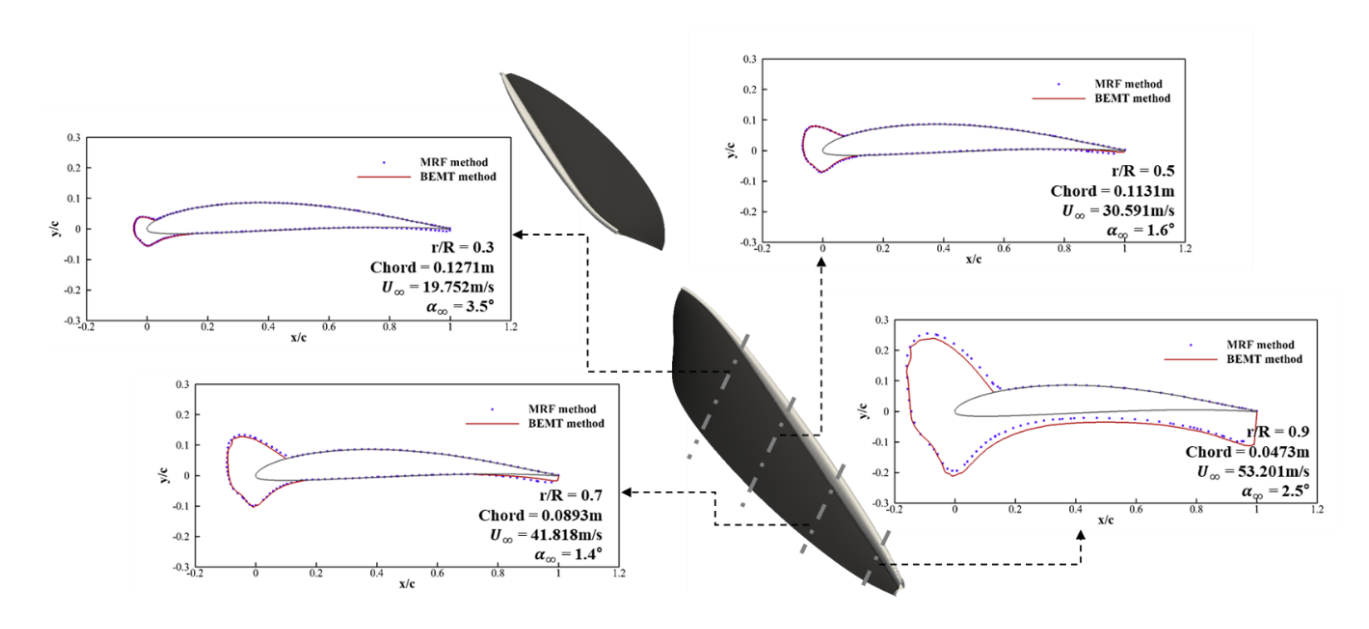


Figure 8 – Comparison of ice shape on each sectional area in rime ice condition (Case 1).

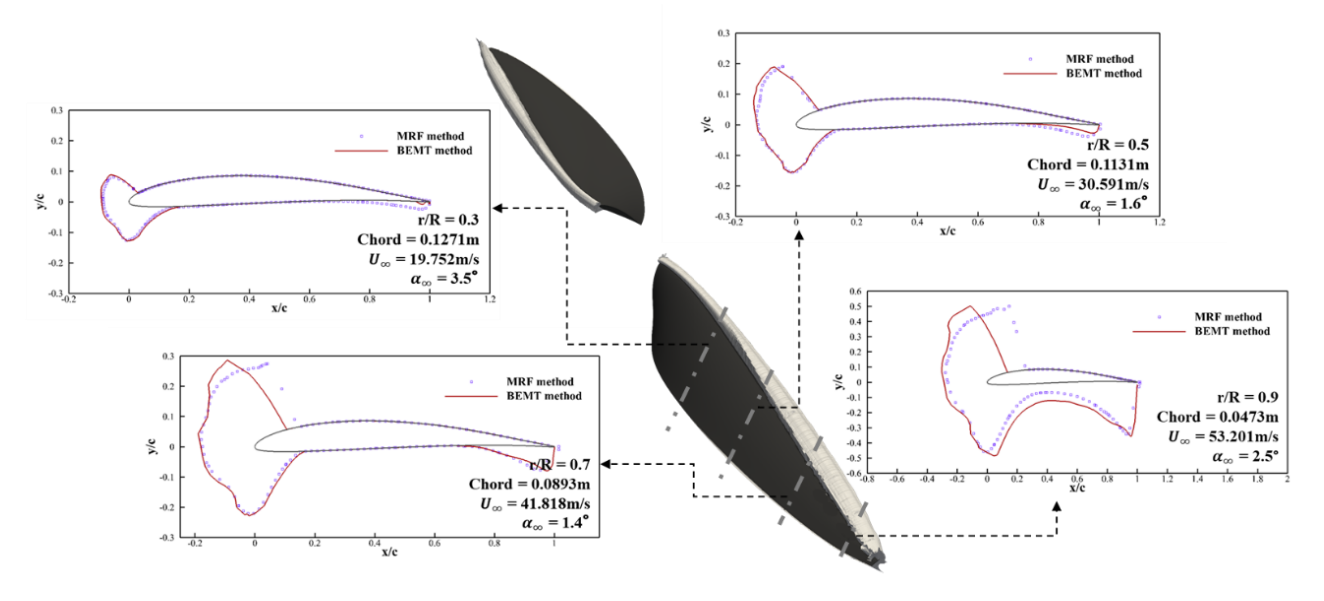


Figure 9 - Comparison of ice shape on each sectional area in glaze ice condition (Case 3).

3.3 Performance Analysis

The icing observed on the propeller is more pronounced compared to that on the fuselage and wings. Figure 10 presents the results of interpreting the performance degradation based on the obtained icing geometry. In terms of weight, it was found that the propeller's size is relatively small compared to the size of the aircraft. As a result, the overall amount of icing on the propeller is not significant, and its effect is accordingly limited, as illustrated in Figure 10(a). However, as shown in Figure 8 and 9, the change in the propeller geometry due to icing is substantial. This change leads to a degradation in the performance of the propeller, as shown in Figure 10(b).

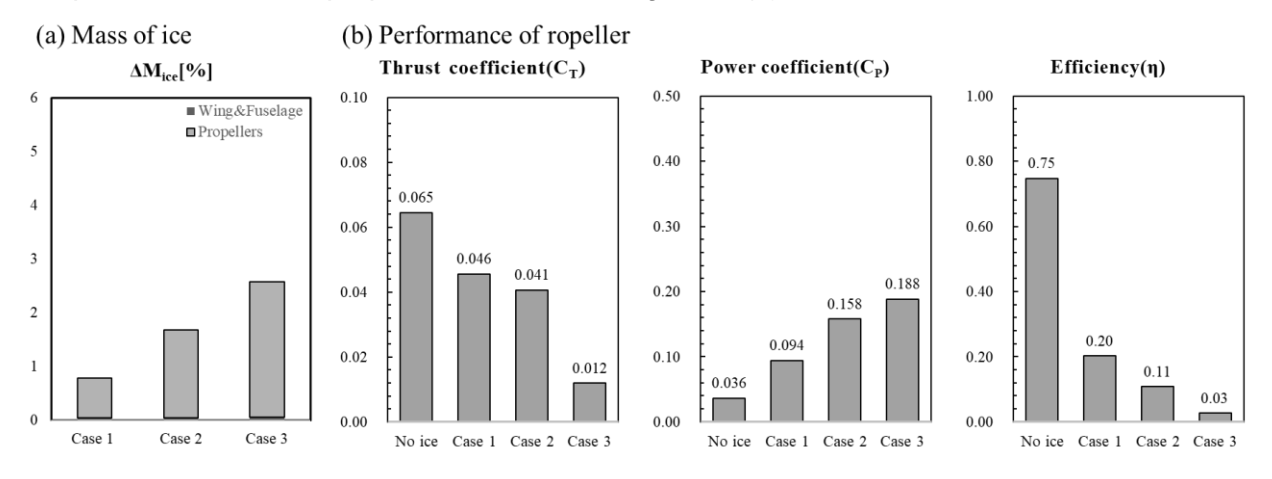


Figure 10 – Performance degradation of EAV-3 due to icing.

3.4 Assessment Operational Limits

In icing conditions, both the fuselage, wings, and the propeller experience performance reduction, which is critical to assessing whether the mission altitude of a HALE UAV can be achieved. Thus, we estimated the required battery capacity, RPM, and torque for the DC motor based on the mission altitude, accounting for performance degradation due to icing, as shown in Figure 11 and 12.

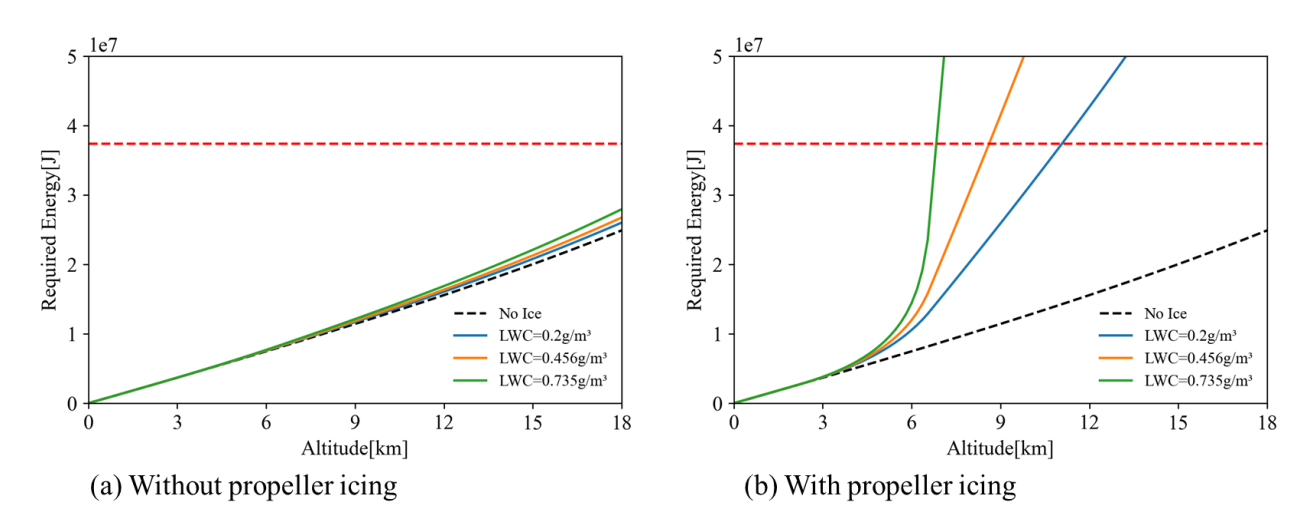


Figure 11 – Required Energy of EAV-3.

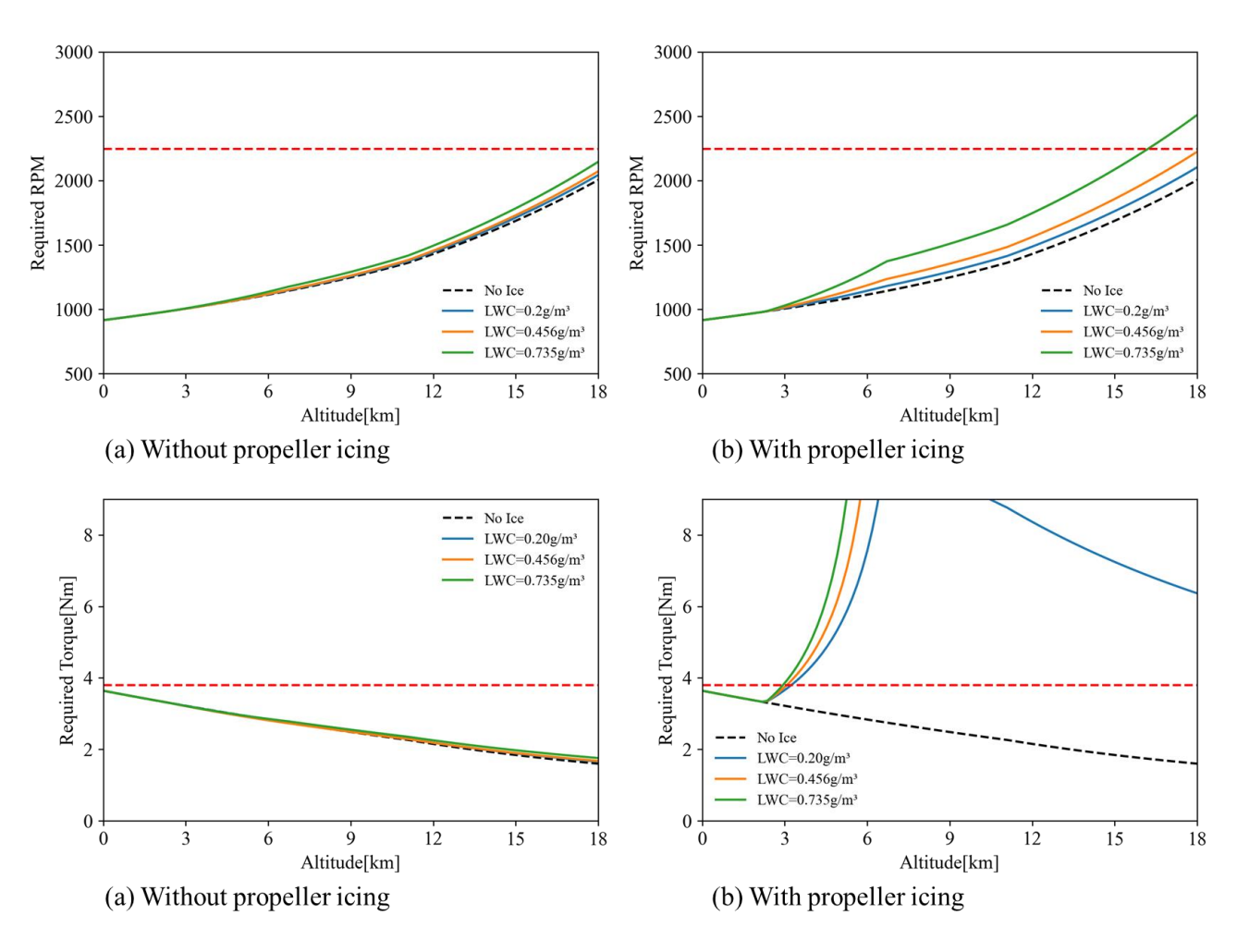


Figure 12 - Required RPM(top) and torque(bottom) of EAV-3.

Firstly, Figure 11 illustrates the required battery capacity as a function of altitude. It shows an increase in required energy from 2.3 km to 6.7 km, where icing conditions occur. Importantly, the figure indicates that without considering propeller icing, the total battery capacity required for the EAV-3 remains within acceptable limits. However, when propeller icing is factored in, the cumulative demand exceeds the battery capacity limit, preventing the UAV from reaching the mission altitude.

Similarly, Figure 12 illustrates the required RPM and torque for a DC motor. Like battery capacity, the required RPM increases with altitude, and icing can lead to exceeding the maximum RPM, thereby preventing reaching the mission altitude. The required torque is typically highest at sea level due to higher air density. However, in the presence of icing, the required torque increases significantly, surpassing the maximum torque and resulting in failure to achieve the mission altitude. In both cases—battery capacity and DC motor performance—the impact of icing is magnified by higher Liquid Water Content (LWC), making it increasingly challenging to attain the mission altitude. These findings collectively demonstrate that icing across all altitude ranges where it can occur leads to mission failure, particularly when considering propeller icing.

4. Conclusion

This study explored the impact of icing on High-Altitude Long Endurance Unmanned Aerial Vehicles (HALE UAVs), focusing particularly on propeller icing. Independent 3D icing simulations were conducted for both the fuselage/wings and the propellers using the Multiple Reference Frame (MRF) method to account for rotational effects. The findings revealed that propeller aerodynamic performance is significantly compromised compared to that of the fuselage and wings under icing conditions. Based on the degradation in performance caused by icing, the study assessed the feasibility of reaching the mission altitude. It underscored the criticality of considering propeller icing to ensure the safe operation of HALE UAVs, especially concerning the limitations imposed by battery capacities and DC motors.

The study concludes that, assuming all of icing occurs within the relevant altitude range, the EAV-3 UAV cannot achieve its mission altitude due to propeller icing. This underscores the critical need for effective mitigation strategies and design considerations to manage the adverse effects of icing on UAV operations.

5. Contact Author Email Address

kjyee@snu.ac.kr

6. Copyright Statement

The authors confirm that they, and/or their company or organization, hold copyright on all of the original material included in this paper. The authors also confirm that they have obtained permission, from the copyright holder of any third party material included in this paper, to publish it as part of their paper. The authors confirm that they give permission, or have obtained permission from the copyright holder of this paper, for the publication and distribution of this paper as part of the ICAS proceedings or as individual off-prints from the proceedings.

References

- [1] Vogel, G. N. Icing Considerations for HALE (High Altitude, Long Endurance) Aircraft. *Naval Environmental Prediction Research Facility*, Rept. NEPRF-TR-88-11, 1988.
- [2] IYA, S., and COOK, D. Icing characteristics of a high-altitude long-endurance aircraft wing airfoil. 29th Aerospace Sciences Meeting, 1991.
- [3] Bottyán, Z. In-flight icing characteristics of unmanned aerial vehicles during special atmospheric condition over the carpathian-basin. *ACTA Geographica Debrecina Landscape and Environment* 7.2, 2014.
- [4] Son, C., and Yee, K. Procedure for determining operation limits of high-altitude long-endurance aircraft under icing conditions. *Journal of Aircraft*, Vol. 55, No. 1, 2018.
- [5] Son, C., Oh, S., and Yee, K. Ice accretion on helicopter fuselage considering rotor-wake effects. *Journal of Aircraft*, Vol. 54, No. 2, 2017.
- [6] Bourgault, Y., Beaugendre, H., and Habashi, W. G. Development of a shallow-water icing model in FENSAP-ICE. *Journal of Aircraft*, Vol. 37, No. 4, 2000.
- [7] Son, C., and Kim, T. Development of an icing simulation code for rotating wind turbines. *Journal of Wind Engineering and Industrial Aerodynamics*, Vol. 203, No. 104239, 2020.
- [8] Leishman, G. J. Principles of helicopter aerodynamics with CD extra. Cambridge university press, 2006.
- [9] Nakakita, K., Nadarajah, S., and Habashi, W. G. Toward real-time aero-icing simulation of complete aircraft via FENSAP-ICE. *Journal of Aircraft*, Vol. 47, No. 1, 2010.
- [10]Lee, J. D., Harding, R., and Palko, R. L. Documentation of ice shapes on the main rotor of a UH-1H helicopter in hover. No. NASA-CR-168332, 1984.
- [11]Fouladi, H. Computational methods for rotorcraft icing. McGill University(Canada), 2016.
- [12] Hwang, S. J., Kim, S. G., Kim, C. W., and Lee, Y. G. Aerodynamic design of the solar-powered high altitude long endurance (HALE) unmanned aerial vehicle (UAV). *International Journal of Aeronautical and Space Sciences*, Vol. 17, No. 1, 2016.
- [13] Park, D., Cho, T., Kim, C., Kim, Y., and Lee, Y. Performance evaluation of propeller for high altitude by using experiment and computational analysis. *Journal of the Korean Society for Aeronautical & Space Sciences*, Vol. 43, No. 12, 2015.
- [14] Federal Aviation Regulations. *Part 25-Airworthiness Standards: Transport Category Airplanes.* Code of Federal Regulations, U.S. Department of Transportation, Federal Aviation Admin., Washington, D.C..